北海道大学工学部研究報告
第120号（昭和59年）

Bulletin of the Faculty of Engineering,
Hokkaido University, No. 120 (1984)

D-T Fusion Neutron Irradiation of Materials with Rotating Target Neutron Source RTNS-II

Michio KIRITANI

(Received November 30, 1983)

Abstract

Procedure and results of the first experiment of D-T fusion neutron irradiation of materials with the rotating target neutron source RTNS-II at LLNL, performed under the Japan-US cooperation proagrom of fusion research, are described. Materials irradiated are mainly metals and alloys, including some semiconductors and insulators. Results include; neutron collision cross-section to produce survived defects, size distribution of the defects, indication of the existence of sub-cascade damage, observation of disordered zones, formation of metastable defects in a semiconductor, and the role of free interstitials.

1. Introduction

Irradiation of materials with RTNS-II D-T fusion neutron source (Rotating Target Neutron Source-II) at Lawrence Livermore National Laboratory has been approved as one of the priority experiments of the Japan-US cooperative research program started in 1982. This report will give the survey of the procedure and the obtained results of the first experiment conducted during the summer of 1982.

The experimental research plan was made on the understanding that this world strongest rotating target neutron source is not strong enough to test the materials up to the stage of the practical fusion environment but is sufficiently strong to aquire fundamental understanding of the characteristic of radiation damage by fusion neutrons. Another factor which has been strongly considered in the planning was to effectively utilize this first experimental run to make all the related Japanese scientists acquainted with this experimental method for the purpose of the prospective work in the near future. From these two considerations, the material samples included in this experimental program were expanded to a wide variety of materials including the present day candidate materials for fusion reactors.

The principal method adopted is the observation of micro-structure change by neutron irradiation with transmission electron microscopy, and the present principal investigator has been appointed as one of the experienced scientists both in the related field of research and in the experimental techniques.

2. Specimens Prepared and Materials Irradiated

Materials and thier treatments of specimens prepared for the irradiation are listed in Table 1. Objectives of each given treatment are multipurpose, and their examples are; (1) detection of free defects from the change of pre-existing defects, (2) influence on cascade

Department of Precision Engineering

Table. 1 Materials and treatments of samples irradiated

	Material	Treatment
1	Al	Annealed
2	Al	Cold owrked
3	Al	Doped with V-dislocation loops by quenching
4	Al	Doped with voids by quenching
5	Al	Doped with I-dislocation loops by electron irradiation
6	Al-dilute alloys	Ag & Si up to 500 at. ppm
7	Cl-Cu	With GP zones
8	Au	Annealed
9	Au	Doped with stacking fault terahedra by quenching
10	Au	Annealed
11	Fe	Cold Worked
12	Fe	Pre-irradiated with electrons
13	Fe-C	Solution treated
14	Ge	Single crystal
15	MgO	As grown
16	MgO	Purified
17	Ni	Annealed
18	Ni	Cold worked
19	Ni	Doped with I-dislocation loops by electron irradiation
20	Ni	Doped with voids and bubbles by ion irradiation
21	Ni	He ion pre-irradiated
22	Mo	Cold worked
23	Mo	Pre-irradiated with electrons
24	V	Cold worked
25	V-C	Solution treated
26	V-C	ϵ-phase Precipitated
27	Cu_3Au	Ordered
28	Ni_3Al	Ordered
29	NiAl	Ordered
30	FeAl	Ordered
31	TiNi	Ordered
32	NiC	Near stoichiometry
33	Fe-Cr	Various compositions with and without C
34	Fe-Cr-Ni	〃 〃 〃 〃
35	Fe-Cr-Mo	〃 〃 〃 〃
36	Fe-Cr-Nb	〃 〃 〃 〃
37	Fe-Cr-Ti	〃 〃 〃 〃
38	Fe-Cr-Ni-Ti	〃 〃 〃 〃
39	316 SS	Variously modified
40	Ferritic steels	Ferrite only
41	Ferritic steels	Ferrite and martensites
42	Amorphous FeB	14, 20 and 25 at.% B
43	Polimers	3 kinds
44	SiO_2	For optical measuremnts

stability by pre-existing defects, (3) effect on cascade stability by minor elements, (4) application of order diffraction observation, (5) detection of the difference in various metallurgical phases, and (6) variation of cascade stability with characteristic temperature of point defects.

Almost half of the total 200 loaded samples were pre-thinned for electron microscope

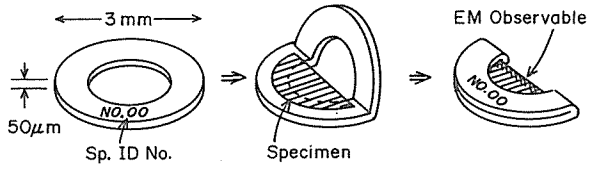

Fig. 1 Mounting of thin foil specimen with aluminum thin plate. The purpose is to minimuze specimen mass to avoid the residual radio-activity.

observation, and two-thirds of the pre-thinned samples were sandwiched between thin aluminum half-disks as in Fig. 1 to minimize the induced radio-activity by having the

possible smallest mass of deleterious materials (less than 0.005 mg for each). Others were standard 3 mm disks, some jet polished and others not. Numbers of samples, especially those which were given specific treatments, were observed with an electron microscope before the irradiation and their characteristic structures were recorded.

Polymers and ceramics, whose immediate purpose of experiment was in optical measurement, were in the shape of 10 mm × 6.5 mm with a thickness from 0.1 to 0.5 mm.

3. Irradiation Chamber and Sample Loading

In order to prevent contamination and oxidation of samples after their preparation till the end of the irradiation before observation, a compact vaccum sealed chamber was designed and constructed . Figure 2 (a) shows its disassembled illustration and Fig. 2 (b)

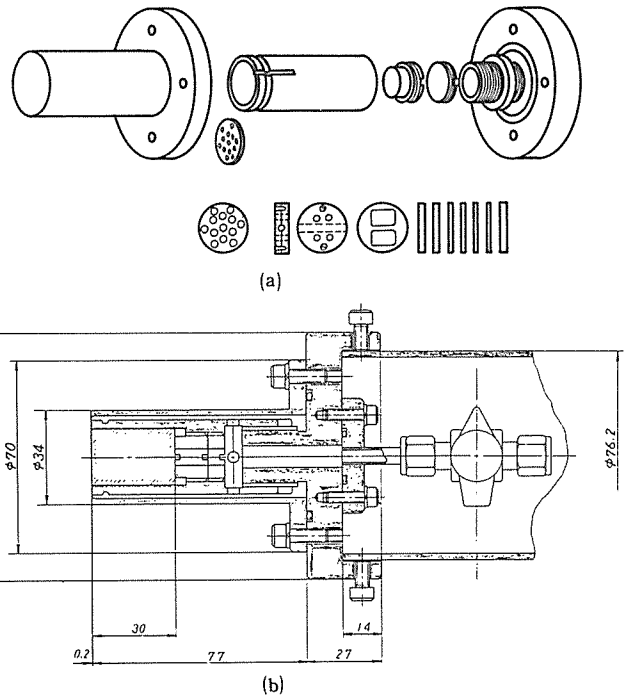

Fig. 2 Schematic disassembled view of the vaccum irradiation chamber (a), and its real dimension (b).

shows its real dimension. Figure 3 shows the component parts of the chamber. Its functions considered are; (1) to locate the samples as close as possible to the target, the front window was made as thin as possible (~200 μm), (2) a large number of specimens can be loaded in several separate capsules which have holes to fit 3 mmϕ specimens, (3) one of the capsules was designed in such a way as to place specimens parallel to the neutron beam, (4) adjustability of the front specimen position to touch and support the front window, and (5) to minimize the induced radio-activity, aluminum (6061) was used for all the parts of the chamber,. In this chamber, more than 50 TEM disk specimens could be contained within a thickness of 1 mm and within a diameter of 17 mm.

200 specimens were loaded in one vaccum chamber together with 36 Fe and Nb

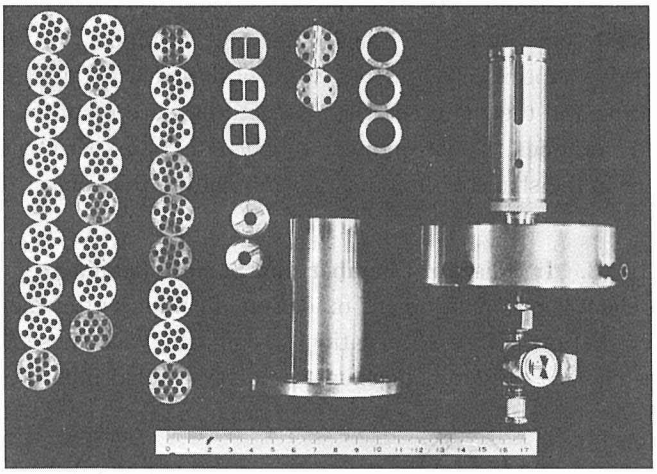

Fig. 3 Component parts of the vaccum chamber for irradiation.

dosimetry foils. Two sets of the complete chambers loaded with identidal specimens were prepared. The second set was for the purpose of replacement of the first one in case of a mishap, and also for the comparison experiment with fission neutron irradiation when not used for RTNS-II. Fortunately, the second set was not irradiated at LLNL, and it was irradiated by fission neutrons at the Research Reactor Institute of Kyoto University.

4. Irradiation with RTNS-II

The irradiation was continued for complete 3 weeks, every day 15 hours, 5 days a week, using a newly installed 50 cmϕ target. By this irradiation the neutron fluence on the dosimetry foil placed at the center of the chamber window out-side the chamber reached 1×10^{18}n/cm^2.

The radio-activity measured at two and half days after the completion of the irradiation was as strong as 80 Rem/h at a distance of about one inch from the center of the tip of the chamber, but further measurements for several days definitely indicated that the major activity was from the required for the aluminum composing the chamber. Five days of cooling enabled handling disassembling the chamber and the start of electron microscope observation.

The neutron fluence on each specimen was estimated within the acceptable error from the fluence measured on 36 dosimetry foils placed at appropriate positions in the irradiation chamber. The dosimetry was carried out by the Dosimetry Department of LLNL. Figure 4 shows examples of the fluence map as the function of the length distance Z from the window, radial distance r from the central axis of the chamber and the rotating angle θ. Variation of the fluence with a wavy shape against the rotating angle at fixed Z and r indicates the strongest center of the neutron source was shifted from the center of the specimen chamber. The shift was estimated to be about 4 mm.

5. Electron Microscope and Other Instrumentation

A high resolution electron microscope Model JEM-200CX was installed in RTNS-II Laboratory especially for the purpose of usage in the present research program, and it was

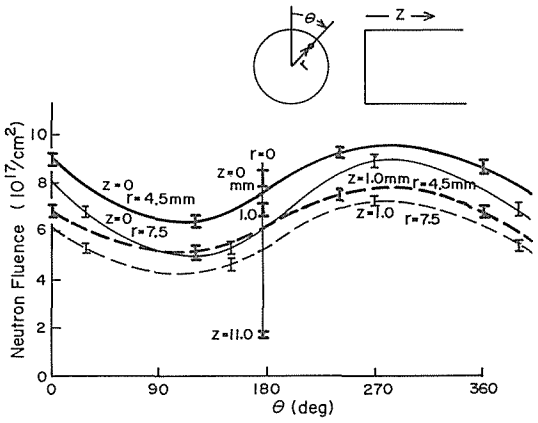

Fig. 4 Distribution of the neutron fluence obtained from the induced radio-activity of the dosimetry foils.

demonstrated that the required performance of 1.4 A resolution could be obtained. A double tilt specimen holder, Type BST3 and a double tilt specimen heating holder, Type SHTH, with a heating power unit and a temperature measurement device were also attached.

Two sets of jet polishing equipments, TENUPOLE, were supplied for the post-irradiation specimen polishing, and a high vaccum evaporation chamber, Model JEM-5B, was installed. Inevitable installation of a photographic dark room was finished during the period of the irradiation. The dark room facility fullfiled the minimum requirement for electron microscopy.

6. Brief Description of the Observed Results and Discussion

Observation of about 40 specimens, for which the induced radio-activity could not be expected to cool down within one month to the level of non-active materials, were performed at RTNS-II Laboratory, and more than 1000 EM photographs were carried back to be analyzed by each research participant. About 50 specimens whose activity was originally very weak or cooled down sufficiently are now under observation in Japan. Observation techniques adopted for each purpose were; (1) observation at various specimen thickness, with thickness measurement, to obtain the numerical data of the number density of defects, (2) weak beam dark field observation to detect the size and the shape morphology of small defects, (3) stereoscopic observation to obtain three dimensional distribution of defects, (4) 2 1/2 dimension observation to identify the character of defects, (5) order-reflection dark field observation to detect disordered zones for the materials applicable, and (6) lattice image observation for some specific materials.

6-1. Number density of survived defects

One of the most reliable methods to obtain volume number density of defect clusters is to measure the projected areal number density as the function of specimen thickness, and this method was applied for all materials in which observable defects survived after the irradiation.

Figure 5 is an example of nickel showing equal thickness fringes on a tapered specimen edge to the left and the dark field weak beam electron microscope image of the same area to the right. The gradient of the measured areal number density against the specimen thickness as in Fig. 6 gives the volume number density. The cases in the figure gives the defect number density of $4.0\times10^{17}/cm^3$ for Ni and $1.9\times10^{17}/cm^3$ for Au.

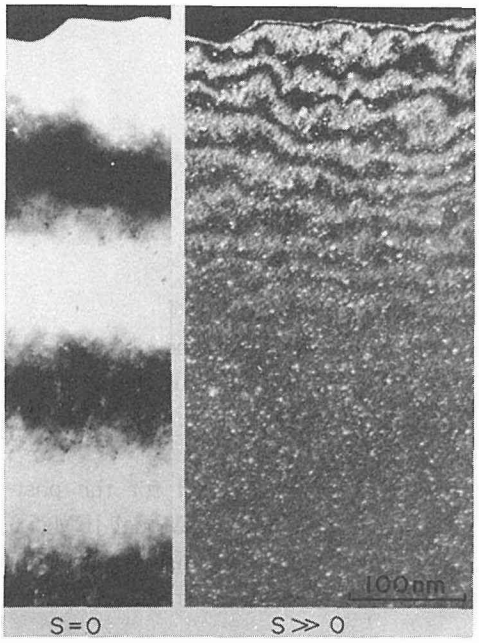

Fig. 5 Measurement of the number density of defects. The case of Ni, $7.7\times10^{17}n/cm^2$. Specimen thickness is measured from the equal thickness fringes on the left, and areal number density is obtained from the weak beam electron microscope image on the right.

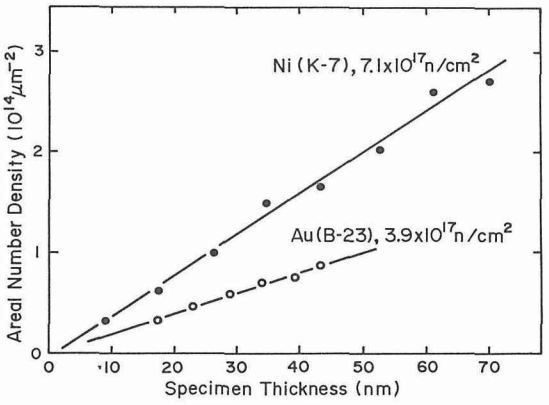

Fig. 6 Areal number density of defects plotted against the specimen thickness. The gradient gives the volume number density.

From the measured volume number density of defects and measured neutron fluence, the free path length of neutrons between collisions which produce such vacancy clusters can be estimated. The estimated values from the experimental data of the room temperature irradiation are 13, 3, 11 and 9 cm for Au, Ni, Cu_3Au and Ge, respectively. These can be converted to the cross-section of neutron collision to produce survived vacancy type clustered defects, and these are 1.3, 3.9, 1.2 and 2.6 barns, respectively.

The above data were obtained from the observation of thin specimens (thickness$\lesssim$100 nm) all pre-prepared for the transmission electron microscopy prior to the irradiation. This procedure is important to prevent the destruction of once formed vacancy clusters by interstitials as will be discussed later as the role of free interstitials. Strict linear increase of the observed areal number density in Fig. 6 with the specimen thickness proves that no effect of free interstitials exists at least for the number density in this range of specimen thickness.

6-2. Size distribution of defects produced from cascade damage

Size distribution of the survived defects can be obtained from the highly magnified electron micrographs as in Fig. 7. Figure 8 is an example obtained for pure Ni, and it has

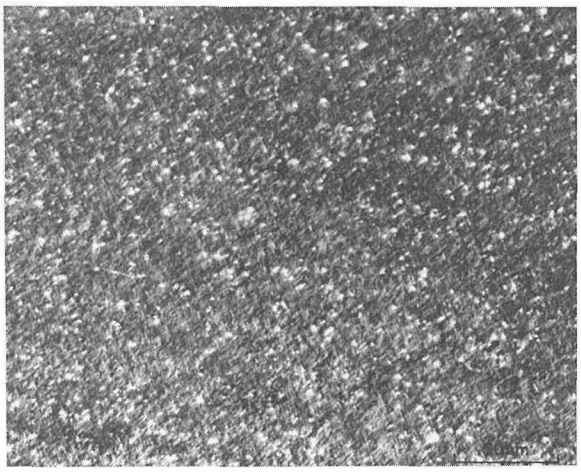

Fig. 7 Defects formed in nickel. 7.7×10^{17}n/cm^2.

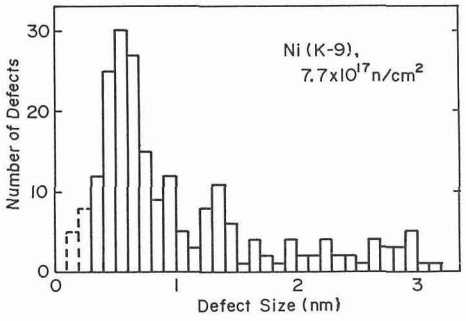

Fig. 8 Size distribution of defects formed in Ni. 7.7×10^{17}n/cm^2.

a long tail elongated towards the larger size. The size distribution of disordered zones which will be described later has a different shape with smaller tail. These should be discussed from the distribution of the transfered energy and displacement mechanism.

In order to discuss the size of vacancy clustered defects directly formed from the cascade damage, the data should be obtained from the specimens thinned prior to the irradiation, in which the change of the defect size by the absorption of free interstitials released from other cascades is prevented.

6-3. Sub-cascade damage

Several observations which are strongly suspected to be the effect of sub-cascade damage are shown in three figures in Fig. 9. Especially the case (a) of gold in which small defects are not distributed randomly but have a strong tendency to make groups up to about ten small dots. Figure 10 (a) is an example of the distribution of the size of the sub-cascade groups counted by the number of sub-cascades contained. Figure 10 (6) shows the distribution of individual defects in sub-cascade groups, which was obtained by multiplying the number of sub-cascades in each sub-cascade group to the number of the groups, and this figure indicates that the major part of defects belong to the sub-cascade groups.

6-4. Defects and disordered zones formed in ordered alloys

Only one system of materials reveal at present the trace of displacement of atoms even without accompanying defect structures, that is the ordered alloys and they have been used efficiently for the damage analysis by English and Jenkins.[1)]

Figure 11 is the electron microscope image of structure change by D-T neutron irradiation in ordered alloy Cu_3Au observed with a variety of imaging conditions. Disordered zones can be observed by the dark field observation with order electron

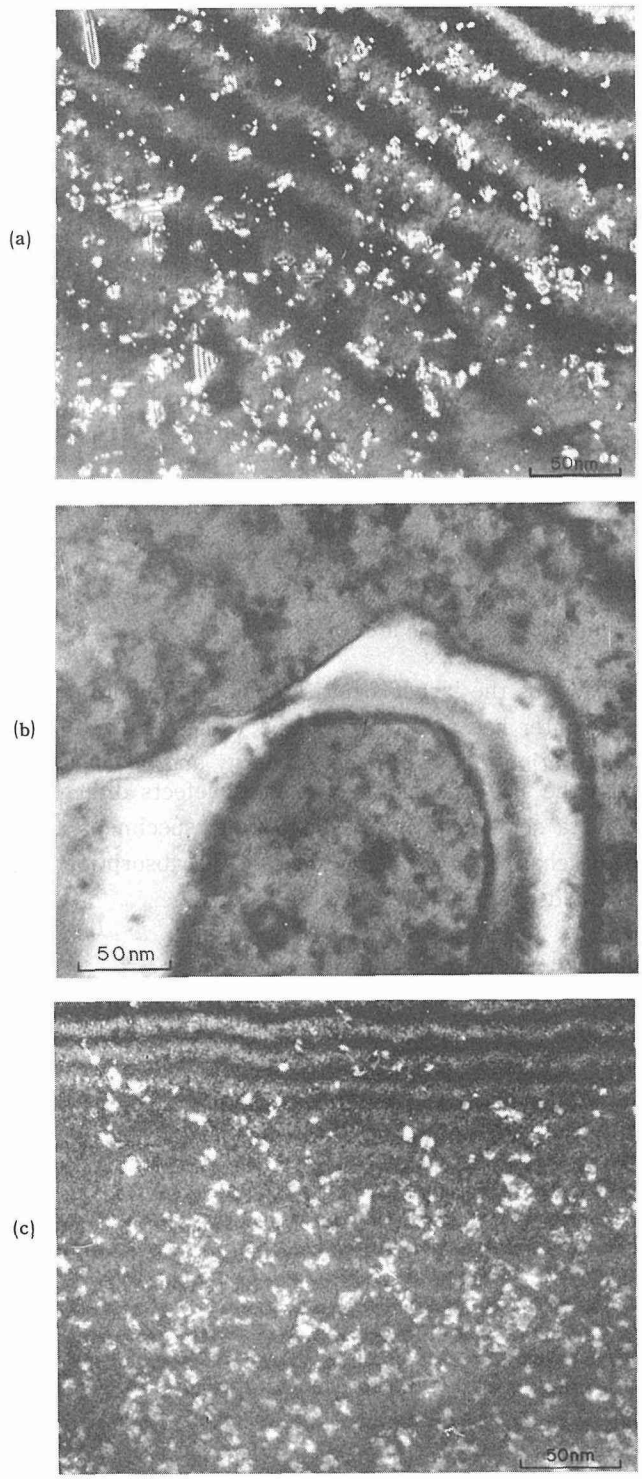

Fig. 9 Defect structures suggesting the existence of sub-cascade damage by D-T neutrons. (a) gold, $3.6\times,0^{17}$n/cm^2, (b) Cu_3Au, 1.8×10^{17}n/cm^2, and (c) Ge, 7.9×10^{17}n/cm^2, all irradiated at room temperature.

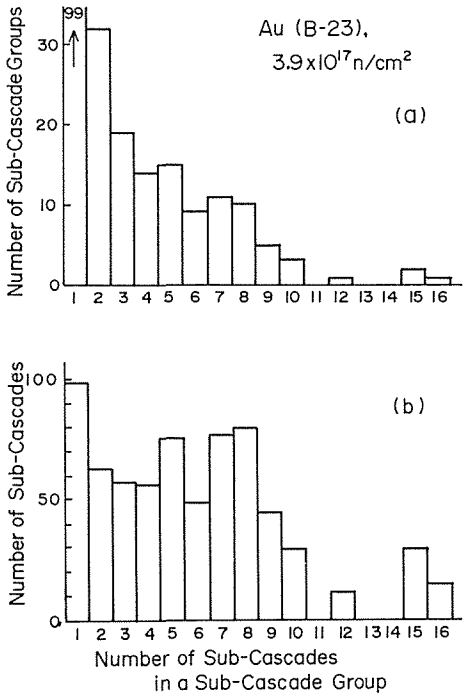

Fig. 10 Numbers of sub-cascades in cascade damage in gold (a), and the distribution of individual defects in cascade groups (b).

reflection, and clustered defects of point defects are observed with normal reflection.

One example of the size and spatial correlation of the survived defects with disordered zones is shown in Fig. 12, in which the areas surrounded by the zig-zag lines indicate the disordered zones and black dots the structural defects. The defects are much smaller than that of disordered zones, and this indicates that interstitial atoms were transported a fairly long distance (~20 nm) away from the vacancy rich central zones by the replacement sequence collision process, forming the disordered atom rows along its paths. Many of the disordered zones are not accompanied by defects, but there might be invisible defects because of the out-of-contrast diffraction condition. Detailed analysis of this kind of observed data gives us the as-damaged distribution of the point defects.

6-5. Metastable defects formed in semiconductors

Well defined defects formed in semiconductor germanium by electron irradiation are interstitial and vacancy type dislocation loops, and they are thermally stable up to the temperature about 400°C.[2)]

The defects formed in the material by the neutron irradiation, whose enlarged images were shown in in Fig. 9 (c), were found to shrink and disappear during room temperature observation under electron microscope as in Fig. 13. The variation of the shrinkage speed with the illumination intensity of electrons showed that the process is not caused by the increase of the specimen temperature but by the radiation-induced type of athermal motion or rearrangement of defect-like structures.

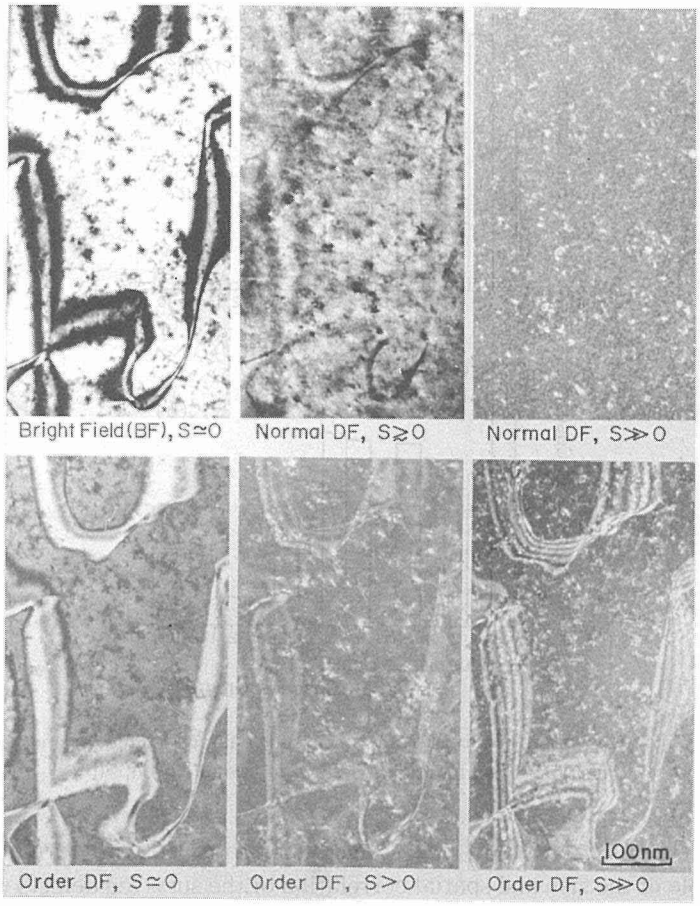

Fig. 11 Electron microscope images of the same area of ordared Cu_3Au observed wiht various electron diffraction conditions. 1.8×10^{17}n/cm^2.

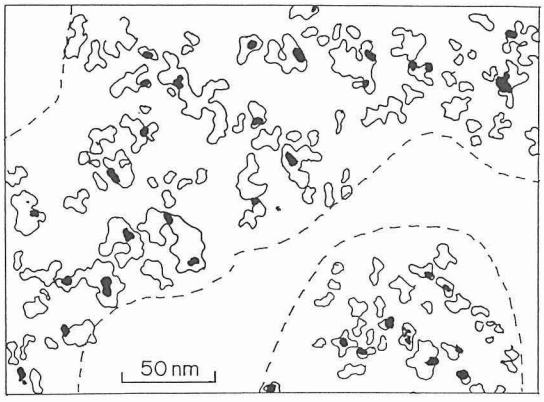

Fig. 12 Spatial and size correlation betwen disordered zones (surrounded by line profiles) and structural defects (black dotts) in D-T neutron irradiated Cu_3Au.

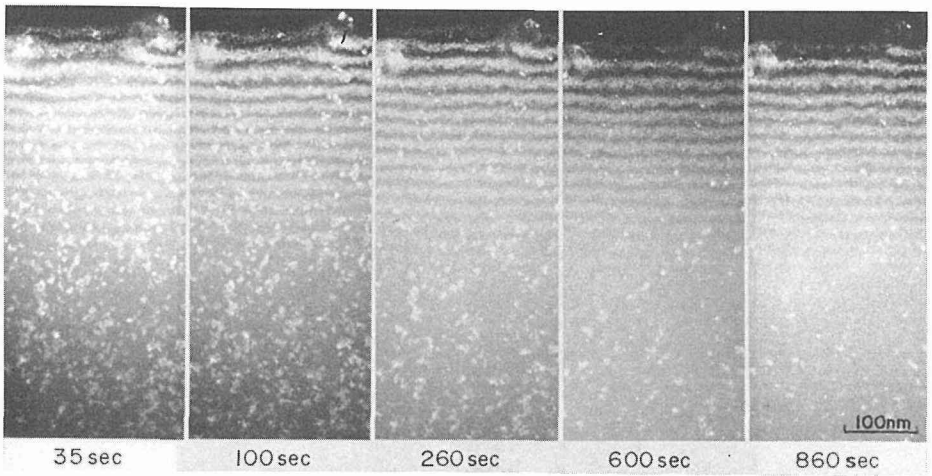

Fig. 13 Shrinkage and disappearance of defects formed by D-T neutron irradiation in germanium during observation with 200 keV electrons.

The atomistic structure of the above disordered zones in germanium has not yet been disclosed, but it can be suspected as the assembly of paritially broken bonds or in extreme the zone of amorphous structure. More knowledge is required on the structure and stability of these defects, for the development of electronic devices and radiation detectors which can be used in the radiation environment.

6-6. Escape of interstitials out from specimen and its relevance to vacancy cluster formation

An astonishingly large difference was found in the vacancy clustered defect formation between the irradiations of pre-thinned specimen suitable for electron microscope observation (<100 nm thick) and bulk specimen observed by thinning after the irradiation. Fig. 14 is the case of nickel irradiated at room temperature. Number dnsity of small dotted defects is far smaller in the bulk specimens showing the effect of destruction by interstitials released from other cascades, on the other hand the interstitials in the thin foil are believed to have escaped promptly to specimen surfaces. Larger defects observed in the bulk irradiation are interstitial clusters.

Another example of the results of the prompt escape of interstitials is shown in Fig. 15 for nickel, in which voids had been introduced by Ar^+ ion irradiation prior to the D-T neutron irradiation. Enhanced formation of vacancy clusters is clearly observed around each void.

6-7. Interaction of free isterstitials with dislocations

Important reactions of free interstitials are those with dislocations. Interstitials have a strong drift flow along the gradient of dilatational strain field of a dislocation. An entirely opposite situation of the concentration distribution of diffusion elements may arise in this case compared with normal case in which the diffusion to sinks leads to the lower concentration of defects near the sink.

The accelerated flow of interstitials around a dislocation can increase their concentration near dislcoation depending on the dislocation geometry, and leads to the

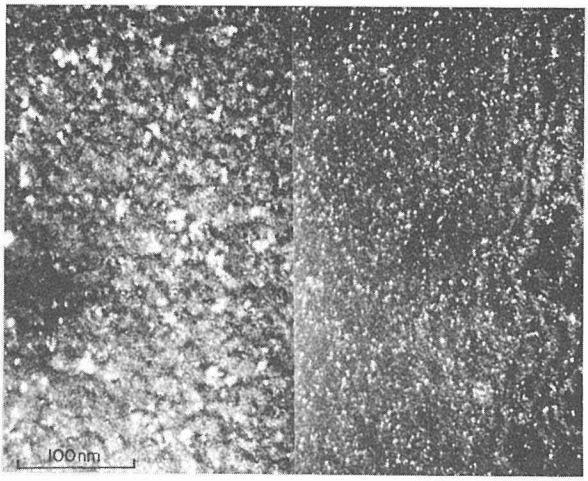

Fig. 14 Difference in clustered defect formation between (a) bulk and (b) thin foil irradiation of nickel at room temprature. Both 6×10^{17}n/cm^2.

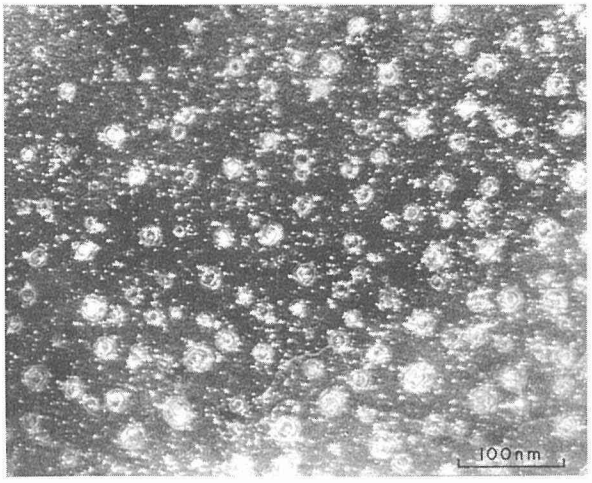

Fig. 15 Enhanced formation of defects around pre-existing voids in nickel at room temperataure. Voids had been introduced by Ar^+ion irradiation.

formation of their clusters in the area immediately adjacent to the dislocation. The defects formed near a dislocation on its one side in Fig. 16 are larger than the vacancy type defects formed in the matrix, and have been identified as interstitial type. This type of interstitial cluster formation is less pronounced when a thin specimen is irradiated, obviously from the escape of interstitials to specimen surfaces.

The decoration of an edge dislocation on its dilatation side with interstitial loops changes the effective strain field distribution around the dislocation, and consequently a consideraction should be given on the change in its bias factor.

7. Concluding Remarks

The majority of the irradiated specimens whose radio-activity is still not low enough

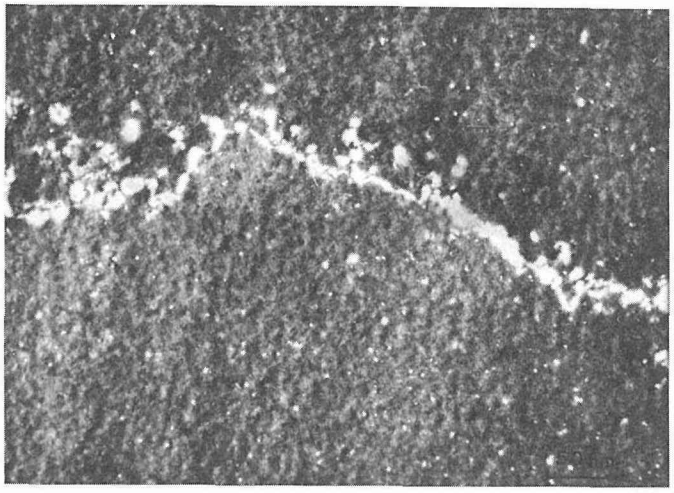

Fig. 16 Interstitial cluster formation near a dislocation in room temperature neutron irradiated nickel. 6×10^{17}n/cm^2.

to be handled freely remains at RTNS-II Laboratory, and they are expected to undergo further examination by scientist in charge who will take the related project research at RTNS-II Laboratory. However, each scientist sent to RTNS-II has his own new research project and naturally can produce more specimens to be observed. In order not to waste valuable specimens and to aim at the effective function of the research project, the most important procedure to be carriedout is to establish a route to send or carry back radioactive specimens to Japanese research institutes which are qualified to hundle various types of examination of irradiated materials. The best and possible plan for this purpose, in the present authors thinking, is to exapand the qualification and the facilities of The Oari Branch, The Research Institute for Iron, Steel and other Metals of Tohoku University.

Acknowledgements

The authors would like to express their gratitude to all those who made this Japan-US cooperative program possible . The author wishes to express his sincere thanks to Professors K. Kawamura and K. Sumita for their valuable and personal encounragement and guidance. He also would like to thank Facility Manager C. M. Logan, Dr. D. W. Heikkinen and all the members of RTNS-II Laboratory, without whose help the present research program could not be carried out. The great help given by Dr. T. Iida through the experiment is highly appreciated.

The author is also grateful to Dr. N. Yoshida, who did the observation on specimens thinned after the irradiation, and for his permission to include the data in this paper.

References

1) English, C. A. and Jenkins, M. L.: J. Nucl. Mater. **96** (1981) 341
2) Hirata, M. and Kiritani, M.: Physica **116 B** (1983) 623.